Pre-operative Screening and Manual Drilling Strategies to Reduce the Risk of Thermal Injury During Minimally Invasive Cochlear Implantation Surgery

Neal P. Dillon,[1] Loris Fichera,[1] Kyle Kesler,[2] M. Geraldine Zuniga,[3] Jason E. Mitchell,[1] Robert J. Webster III,[1,3] and Robert F. Labadie[3]

[1]Department of Mechanical Engineering, Vanderbilt University, 2301 Vanderbilt Place, PMB 401592, Nashville, TN 37240-1592, USA; [2]Vanderbilt University School of Medicine, Nashville, TN, USA; and [3]Department of Otolaryngology, Vanderbilt University Medical Center, 1215 21st Ave. South, MCE 10450, South Tower, Nashville, TN, USA

Associate Editor Jane Grande-Allen oversaw the review of this article.

Abstract—This article presents the development and experimental validation of a methodology to reduce the risk of thermal injury to the facial nerve during minimally invasive cochlear implantation surgery. The first step in this methodology is a pre-operative screening process, in which medical imaging is used to identify those patients that present a significant risk of developing high temperatures at the facial nerve during the drilling phase of the procedure. Such a risk is calculated based on the density of the bone along the drilling path and the thermal conductance between the drilling path and the nerve, and provides a criterion to exclude high-risk patients from receiving the minimally invasive procedure. The second component of the methodology is a drilling strategy for manually-guided drilling near the facial nerve. The strategy utilizes interval drilling and mechanical constraints to enable better control over the procedure and the resulting generation of heat. The approach is tested in fresh cadaver temporal bones using a thermal camera to monitor temperature near the facial nerve. Results indicate that pre-operative screening may successfully exclude high-risk patients and that the proposed drilling strategy enables safe drilling for low-to-moderate risk patients.

INTRODUCTION

Cochlear implants (CI) are the standard of care for restoring the perception of sound to individuals with severe to profound sensorineural hearing loss. These devices bypass the damaged hearing pathway and directly stimulate the auditory nerve through an electrode array that is surgically threaded into the cochlea. Traditional CI surgery requires the removal of a substantial portion of the temporal bone to gain access to the cochlea, as illustrated in Fig. 1. The invasiveness of traditional CI surgery has motivated several research groups to explore alternative, less invasive techniques. One such technique, called the suprameatal approach, was initially proposed by Kronenberg *et al.*[22,23] to provide access to the middle ear through a narrow hole that is drilled blindly from the external surface of the mastoid. The middle ear is then accessed *via* a tympanomeatal flap, enabling both the creation of the cochleostomy and the threading of the array, which is passed to the middle ear *via* the suprameatal tunnel and into the cochlea. To date, this procedure has been performed in more than 500 cases with no report of major complications. However, this approach is limited by the fact that it does not provide an optimal insertion vector into the cochlea, thus making electrode insertion challenging. To overcome this limitation, several research groups have explored the feasibility of drilling the tunnel through the facial recess (see Fig. 1), with the ultimate goal of creating an insertion vector tangent to the basal turn of the scala tympani, i.e. the largest among the cavities that compose the cochlea. The challenge with this approach is represented by the need to operate in proximity of vital anatomy, including the facial nerve and chorda tympani, which can be as close to 0.5 mm to the drilled tunnel. To address this challenge, image guidance

Address correspondence to Neal P. Dillon, Department of Mechanical Engineering, Vanderbilt University, 2301 Vanderbilt Place, PMB 401592, Nashville, TN 37240-1592, USA. Electronic mail: neal.p.dillon@vanderbilt.edu

systems have been used to accurately align the surgical drill with the desired trajectory. Various approaches to this alignment and the subsequent drilling have been proposed, including: patient-specific, bone-attached templates to guide the drill;[3,25] modified industrial robots guided by external tracking systems;[4,28] a custom-developed serial robot that mounts to the patient's bed;[5,6] and bone-attached parallel manipulators.[19–21]

A key difference between the minimally invasive CI systems proposed to date is the method by which the drilling through the temporal bone is performed. Several systems require the surgeon to manually advance the surgical drill along a linear path that is constrained by the patient-specific stereotactic frame, robot, or adjustable mechanism.[3,19–21,25] In other systems, the robot performs the alignment of the drill and the advancement along the desired linear trajectory through the bone.[4–6,28] There are advantages and disadvantages with each approach. The guided manual drilling enables a simpler overall surgical system and keeps the surgeon more directly involved with the process, which better utilizes his/her expertise and may facilitate earlier adoption by clinicians. The automated drilling approach provides better control over the drilling parameters and supports the integration of additional sensors, which enables optimization of the drilling process and redundant safety monitoring.[1,11,32]

A solution being explored by our research group underwent an initial clinical trial, in which the minimally invasive surgical approach was performed on nine patients using customized microstereotactic frames.[24] A major complication of this approach oc-
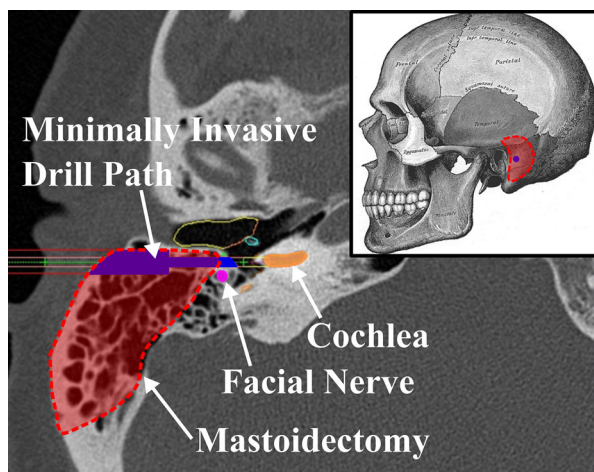

FIGURE 1. Comparison between traditional and minimally invasive approaches to cochlear implantation surgery. The traditional approach requires a mastoidectomy (outlined in dashed line) whereas the minimally invasive approach accesses the middle ear and the cochlea through a narrow drilled tunnel. This tunnel must pass in close proximity to the facial nerve and requires an image-guided device (e.g. robot or stereotactic frame) to safely align the drill.

curred with one patient who experienced immediate post-operative facial nerve weakness and recovered to a House-Brackman score of II/VI[16] after 12 months. Exploratory surgery performed the day after the minimally-invasive procedure was undertaken to explore the facial nerve and it was found to be structurally intact. Thus, we hypothesized that the nerve was damaged by excessive heat secondary to drilling bone near the nerve.

Other groups have explored the potential effect of temperature rises secondary to drilling in more detail. Feldman *et al.* tested a previously developed minimally invasive CI robotic system[5,6] on live sheep and measured the temperature several millimeters from the drilling trajectory using thermocouples inserted into the bone.[11] They then used the acquired temperature data, planned trajectory information, and image data to fit a patient-specific CT image-based thermal model and predicted the temperatures at other locations, including the facial nerve. Their results indicated that temperature elevation is strongly dependent on bone density and dangerously high temperatures are likely to occur for patients with high bone density in the nerve region if safety measures (e.g. irrigation) are not taken, furthering the hypothesis developed by Labadie *et al.*[24] that thermal injury was the likely cause of the facial nerve weakness in the aforementioned clinical trial. Feldman *et al.* performed an additional study to optimize the robotic drilling process for heat reduction.[12] They determined that irrigation and drilling intervals affect temperature elevation and they also designed a custom drill bit that further reduced temperature elevation.

These recent results from Labadie *et al.*[24] and Feldmann *et al.*[11] indicate that controlling the heat generated during drilling in minimally invasive CI surgery is critical for the approach to be a viable alternative to the current clinical standard. The differences between the approaches for drilling the minimally invasive tunnel discussed above (manual vs. automated drill advancement) are particularly relevant for the reduction of heat. It is impossible to control the manual advancement of the drill with precision and consistency comparable to the automated advancement. Thus, to ensure that the manual drilling is executed consistently and safely despite patient anatomical variations and differing levels of surgeon experience, effective safeguards and processes for manual control are required. The purpose of the work presented in this paper is to describe a methodology to perform guided manual drilling for minimally invasive CI surgery such that the risk of causing heat-related damage to the facial nerve is minimized. Included in this methodology are (1) a pre-operative screening process in which individual patient risk is assessed

based on preoperative imaging, i.e. bone density and position of vital anatomy; and (2) novel hardware and a protocol that gives the surgeon better control over the drilling process and the resulting heat generation. An associated experimental setup for the thermal monitoring of the bone near the facial nerve is presented and the drilling protocol is tested on fresh cadaver temporal bones.

MATERIALS AND METHODS

Surgical Approach

The proposed surgical approach to enable safe minimally invasive CI surgery using a manually guided drill consists of two primary components: (1) assessing individual patient risk and (2) safe execution of the drilling near the facial nerve. Figure 2 provides a flow chart of the surgical workflow. The pre-operative risk assessment is used to decide if a patient should undergo the minimally invasive or the traditional approach to CI surgery. A drilling strategy that reduces the risk of temperature rise near the facial nerve is then employed for candidates of the minimally invasive approach.

Pre-operative Risk Assessment

Individual patient risk can be estimated by analyzing the pre-operative CT scan. This risk is dependent on two factors: (1) the amount of heat generated by the drill as it creates the minimally invasive tunnel and (2) how much of that heat spreads to the nerve. Both of these factors are influenced by the density of the temporal bone, which can be calculated from the CT scan and varies considerably within a single patient and between patients. To quantify the risk, we use two metrics as described in detail below to give the surgeon

a basis for deciding whether the patient should undergo the minimally-invasive approach.

While it is likely that the minimally invasive approach could be performed safely on all patients with an appropriate drilling strategy, the manual drill advancement introduces some inconsistency, which could lead to higher temperatures for some patients. Thus, patients that are at high risk should undergo the traditional approach for CI surgery, especially while the minimally invasive approach is in its infancy. A precise temperature prediction cannot be made from the pre-operative data since there will be variability in how the manual drill advancement is performed and effective irrigation at the drilling site is inconsistent. Instead, it is possible to assess the relative risk between patients. Then, if only lower risk patients are considered candidates for the minimally invasive approach, variations in drilling and irrigation that lead to higher temperatures are less likely to result in unsafe temperatures at the nerve.

The amount of heat generated at a given point along the path is a function of the process parameters (e.g. linear velocity, spindle speed, etc.) as well as the bone density at that point,[11] which can be approximated by the CT scan intensity in Hounsfield Units (HU) (see Fig. 3). It is important to note that intensity can vary between scanners and thus yield inconsistent results; the scanners can be calibrated by using test scans with a phantom or by comparing scans of the same patient/specimen. Only the region of bone along the path near the facial nerve needs to be considered in this analysis. Bone has a low thermal conductivity (0.55 W/mK[9]) so heat generated far away from the facial nerve does not result in a high temperature near the nerve. We determined that the region that should be considered is 3 mm lateral and 3 mm medial to the point at which the drill passes closest to the nerve for a total distance of 6 mm. This was calculated by analyzing experimental thermal camera measurements of pilot trials (see experimental methods below). More specifically, the temperature of bone at 3 mm away from the drill position did not increase by more than 3 °C. The bone intensity within a diameter of 1.6 mm (the diameter of the drill bit) is averaged for each point along the path in this region. A simple integral of bone intensity in this critical region can be calculated as:

$$I_{\mathrm{crit}} = \int\limits_{p-3}^{p+3} h(x)\mathrm{d}x$$

where x is the distance along the planned drill path, $h(x)$ is the image intensity at that point, and p is the point on the path at which the drill passes closest to the nerve. To account for the fact that heat generated closer to the nerve has a greater effect on the temper-
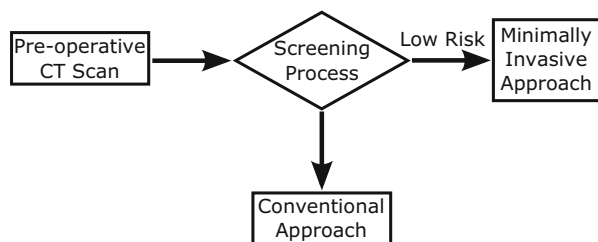

FIGURE 2. Proposed surgical workflow for cochlear implantation (CI) surgery. Patients are screened using their pre-operative CT scan to determine if they at high risk for thermal damage during the minimally invasive approach. High risk patients undergo the traditional approach to CI surgery.

ature of the nerve, the integral can be weighted according to this distance:

$$I'_{\text{crit}} = \frac{1}{K^{\bar{d}}} \int\limits_{p-3}^{p+3} h(x) K^{d(x)} \, dx$$

where $d(x)$ is the distance from the nerve at a given distance along the path, $\bar{d}$ is the mean distance from the nerve for the points considered, and K is the weighting base. In both equations, higher values are associated with greater heat generation and can be used to compare the relative risk of excess heat generated near the nerve between patients

The second risk metric focuses on the composition of bone between the drill path and the facial nerve. Since the mastoid bone contains irregularly sized and shaped air pockets, the thermal conductivity between the drill path and facial nerve varies with bone composition heterogeneity, and leads to a different total thermal resistance between the path and facial nerve for different patients. The conductivity is analyzed by considering a simplified case of one-dimensional heat flow from the point at which the drill passes closest to the nerve and the closest point on the nerve. This calculation is performed by considering a series of cylinders extending from the closest points between the drill path and facial nerve (see Fig. 4). Each cylinder represents a thermal resistance element for one-dimensional conduction between the drill and the nerve. The resistance of each cylindrical element is estimated based on the intensity in the image within that element, which can be correlated with thermal conductivity and
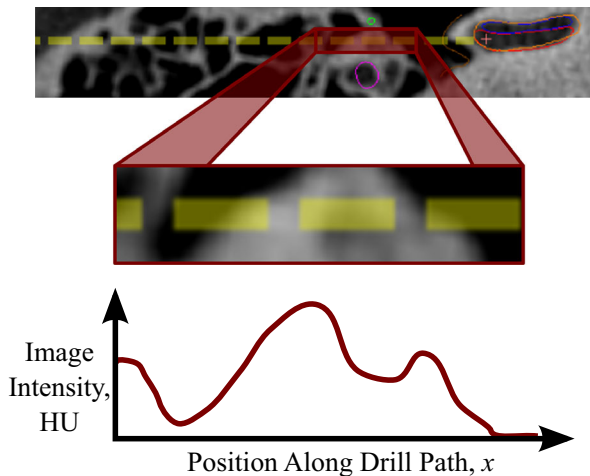
resistance. The thermal conductivity of cortical bone and air are 0.55 W/mK[9] and 0.0269 W/mK (at 37 °C), respectively. The modified intensity values of cortical bone and air (normalized for CT scanner and shifted such that air has a value of 0) are approximately 2500 HU and 0 HU, respectively. Thus, the thermal conductivity of a given voxel or set of voxels in a CT image can be estimated using these values as a reference. Assuming a linear interpolation between the densities of air and bone and their associated thermal conductivities:

$$k_{\text{thermal}} = 0.027 + (2.09 \times 10^{-4})h$$

where h is the image intensity value. The thermal resistance of each cylinder is then computed by:

$$R_{\text{thermal}} = \frac{t}{k_{\text{thermal}} A}$$

where t and A are the cylinder thickness and area, respectively. The total resistance (R_{total}) between the drill path and facial nerve along the series of cylinders is then given by:

$$R_{\text{total}} = R_1 + R_2 + \cdots + R_N$$

where N is the total number of cylinders. The conductance is simply equal to $1/R_{\text{total}}$. The cylinder thickness, which affects the number of cylinders used in this analysis (N), can be selected based on image resolution. For this analysis, a cylinder thickness of 0.1 mm was used (image voxel size ranged between 0.2 and 0.3 mm^3 and was interpolated as necessary). Several cylinder diameters are considered and compared in this analysis, which helps to account for bone composition in the larger region between the path and the nerve as well as the bone along the shortest path to the nerve.

After the two thermal metrics are computed for a given patient, the values are compared to a database of thermal metrics that are calculated from a set of clinical CT scans and drilling trajectories. The difference in scanners is accounted for by analyzing specimens/patients scanned with multiple CT scanners. The relative metric ranking for the patient are then given to the surgeon (e.g. "This patient ranks in the riskiest 44% for intensity along the drill path and in the riskiest 26% for thermal conductance between the drill path and the nerve"). The surgeon can then decide on the appropriate surgical approach for this patient.

FIGURE 3. One of the risk metrics used to evaluate individual patient risk is the integral of the bone intensity along the drill path. A schematic of this metric is shown here. The intensity in Hounsfield units is examined in the area in which the drill path passes close to the facial nerve.

Surgical Drilling Protocol for Reduced Heat Generation

The purpose of this section is to analyze the parameters that can easily be controlled and standardized for the manual drilling approach and subse-

quently propose a drilling strategy to increase the safety and consistency of the procedure. Since the drilling for this surgical approach is performed manually, only a subset of the drilling parameters can be directly controlled. Other parameters, such as feed rate, can be selected in a general sense (e.g. instruct the surgeon to advance the drill at approximately 1 mm/s), but not precisely. Therefore, careful selection of the controllable parameters is critical to minimize the risk of excessive heat generation. Table 1 provides a summary of the proposed manual drilling protocol.

The parameters that define the drilling process are as follows: (1) feed rate, (2) spindle speed of drill, (3) drilling strategy, e.g. continuous drilling vs. peck drilling during which individual pecks are followed by a pause while the drill is retracted and allowed to cool, and (4) irrigation of the bone and drill for cooling. These parameters are discussed individually below.

During manual guided drilling, feed rate and axial thrust force are coupled. In general, higher axial forces and feed rates are recommended for heat reduction.[7] This increases the rate of heat generation but decreases the time of exposure and associated temperature rise. Thus, the surgeon should be in-structed to advance the drill quickly but the drilling strategy must be specified so the total thermal energy generation within a given time period is limited. The drilling strategy employed is an interval drilling approach, which is often used in industrial processes for reduced heat and tool wear.[2,18] Interval drilling in this application provides time for the bone to cool between periods of heat generation. The interval drilling trajectory is defined by two components: depth of each interval and time between intervals. Along with the feed rate, the depth determines the amount of heat generated during each interval. The work of Feldmann *et al.*[12] shows that shorter interval lengths result in lower peak temperatures. Based on this, we constrain each drilling interval in the region near the facial nerve to a depth of 0.75 mm. The drill depth is restricted by a physical stop on the drill slide consisting of a series of disks that are placed on the base of the drill press (see Fig. 5) during the medial drilling stage and prevent drill advancement beyond a given depth. After each drilling interval, the topmost disk is manually removed during the pause between intervals, allowing the drill to travel slightly deeper into the bone for each interval.
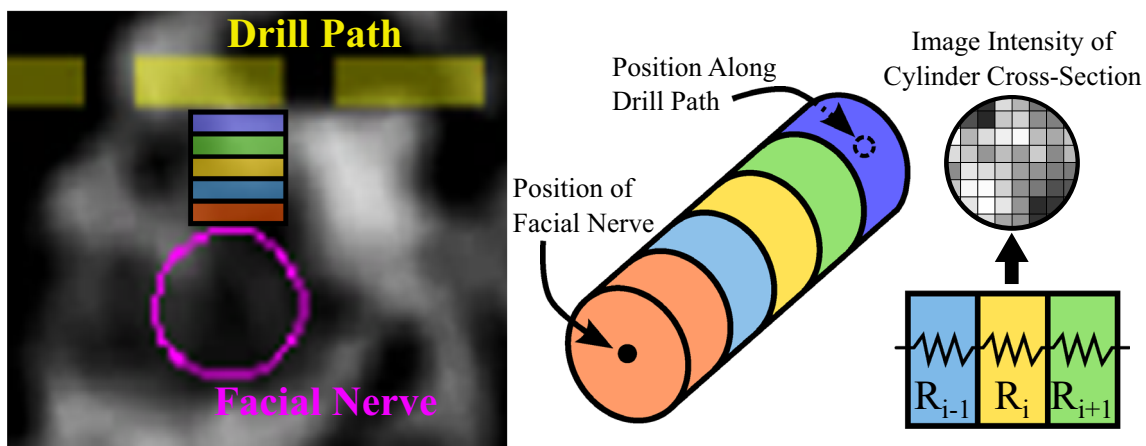

FIGURE 4. Schematic of risk metric related to thermal conductance/resistance between the drill path and the facial nerve. The thermal resistance is considered in a simplified case of one-dimensional heat flow. A series of cylinders are stacked between the point on the drill path that passes closest to the nerve and the nerve. The thermal resistance is calculated according to the image intensity of the cylinder cross section and the known thermal conductivities of solid bone and air. The resistances of each cylinder is then added to get the cumulative resistance.

TABLE 1. Summary of drilling and control mode for manual, guided drilling.

| Parameter	Control mode	Specification
Feed rate	Manual	Approximately 5 mm/s
Spindle speed	Maximum set; manually controlled	≤20,000 rpm
Drilling intervals	Mechanically constrained	0.75 mm per interval
Interval timing	Fixed (timer used)	≥30 s between intervals
Irrigation	Manually administered	Flood hole before/after each interval; cool bit between intervals (18 gauge needle tip)
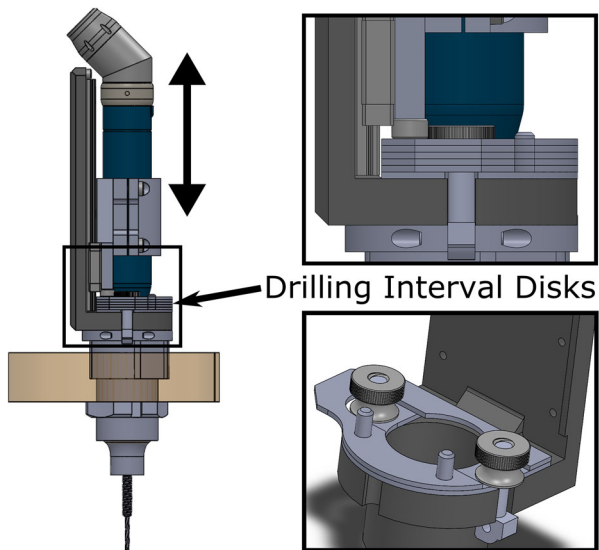
FIGURE 5. Rendering of interval disks for constraining the manually-driven drill press for minimally invasive CI surgery to specified drilling intervals.
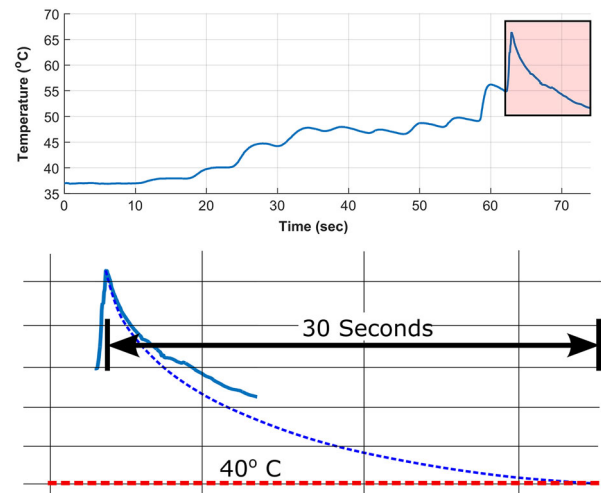

FIGURE 6. Schematic showing estimation of required time between drilling intervals. (Top) Sample pilot data set representing a worst-case scenario, using no irrigation or fixed drilling intervals. The plot shows temperature over time at a distance of 0.5 mm from the facial nerve at the facial recess. (Bottom) The data is cropped around the final drilling interval and overlaid with model data calculated using the thermal model described by Feldmann *et al.*[11] The time required for the temperature to return to within 3 °C of body temperature was calculated to be approximately 30 s. As part of the drilling strategy, we require a pause of at least 30 s between drilling intervals. Note that the model decreases faster since the drill was left in the drilled hole after the peak temperature was reached.

Longer pauses permit more cooling; however, this benefit must be weighed against extending the duration of the surgical procedure. To determine an appropriate time, which we defined as the minimum time needed for the bone located 0.5 mm from the drill surface to return to within approximately 3 °C of base body temperature, experimental measurements of drilling temporal bones were analyzed. Figure 6 shows a schematic of this calculation. Considering a worst-case scenario from pilot data, in which irrigation was not used and temperature rose to over 65 °C, the cool down phase on the last interval was analyzed. The data was extrapolated using a moving point source model[11] and it was determined that the bone temperature would return to within approximately 3 °C of body temperature if left to cool for 30 s between drilling intervals. In typical scenarios where the temperature rise is lower and irrigation is applied, the bone temperature will cool faster and to an even lower temperature.

Recommendations for drill spindle speed vary in the literature; however, it is generally recommended to use lower spindle speeds when possible,[7,26] which helps to reduce the amount of friction between the drill bit and the walls of the drilled tunnel and, in turn, the amount of heat generated. However, standard otologic drills such as the ones used in our system are designed for high spindle speed, low torque operation. Thus, their performance is limited at lower spindle speeds during which the drill can stall easily. To balance the performance limitation with the need for lower spindle speeds, the surgeon should use the lowest rate that enables cutting of bone without stalling the drill. In our current application, the spindle speed is limited to a maximum of 20,000 rpm. However, it is important to note that given the potential for higher temperature elevation associated with higher spindle speeds, a custom drill that fits within the surgical workflow and enables cutting with a higher torque and lower spindle speeds will likely be needed before this approach can achieve widespread use.

Finally, the method of irrigation during the drilling process must be considered. Flood irrigation is used while milling a mastoidectomy during traditional CI surgery. In the minimally invasive approach, irrigating the cutting site is more difficult since the drill bit fits snugly within the hole and tends to pump water out of the hole rather than allow it to travel down to the cutting site. Thus, sufficient irrigation must be provided into the drilled hole between drilling intervals while the bit is removed. It is also important to cool the bit directly and remove any material embedded in the flutes with a higher pressure stream. This can be accomplished by using a narrow (18 gauge) needle at the end of the irrigation tubing. The surgeon must verify that no material is embedded in the flutes of the drill bit before beginning the next drilling interval. If material is embedded and cannot be easily removed, the drill bit should be exchanged for a new one.

Experimental Evaluation of Temperature Rise Near the Facial Nerve

An experimental setup to measure temperature rise near the facial nerve on fresh ex vivo cadaver temporal bone specimens for validation of the proposed strategy was developed using the Microtable system.[25] The temperature measurements were made by cutting the temporal bone specimens such that the bone near the facial nerve could be viewed with a thermal camera from the medial side. To set up each bone for the experiments, a modified version of the surgical planning protocol for the Microtable was performed as follows. Bone anchors and fiducial markers were fixed to the temporal bones and an image was acquired using a conventional CT scanner (Philips iCT, 0.234 × 0.234 × 0.335 mm voxel dimensions). Vital anatomy was automatically segmented[30] and the drilling trajectory from the skull surface to the facial recess was planned on the CT scan.[29] Using the location of the fiducial markers and the planned drill path, the Microtable was then designed, manufactured, assembled and mounted to the fiducial markers on the temporal bone.

Then, by clamping the Microtable and bone to a vise for alignment, the bone was cut along a plane at the facial recess, perpendicular to the drill path, as defined in the CT image (see Fig. 7a) with a diamond-coated band saw. The facial recess was chosen as the plane at which to measure temperature since the drill path passes close to the facial nerve in this area. Furthermore, since there is an air gap in the facial recess and middle ear, a cut at this location does not affect the boundary conditions of the heat transfer of the bone as much as if the cut was made more laterally.

The Microtable was then clamped to a lab bench and an infrared thermal camera (Flir A655sc, Flir Systems, Wilsonville, OR, USA) with a 50 μm close-up lens was positioned at the medial side of the bone to record the bone temperature continuously at the cut plane (Fig. 7b) while drilling. The emissivity constant was set to 0.95 in the Flir software, which lies within the range of the experimentally determined value for bone.[13] The camera was focused on the area of bone through which the drill would subsequently pass a test thermal image was acquired to confirm the bone was in focus. A linear transducer was mounted to the manual drill press to measure the position of the drill during the experimental trial. The thermal and drill position data were exported to MATLAB and the temperature distributions throughout the trajectories were analyzed.

Fresh cadaver temporal bones were obtained from Science Care Inc. (Phoenix, AZ, United States) and 3 drilling trials per bone were performed according to the drilling protocol described in the previous section by an experienced otologic surgeon. For each bone, the
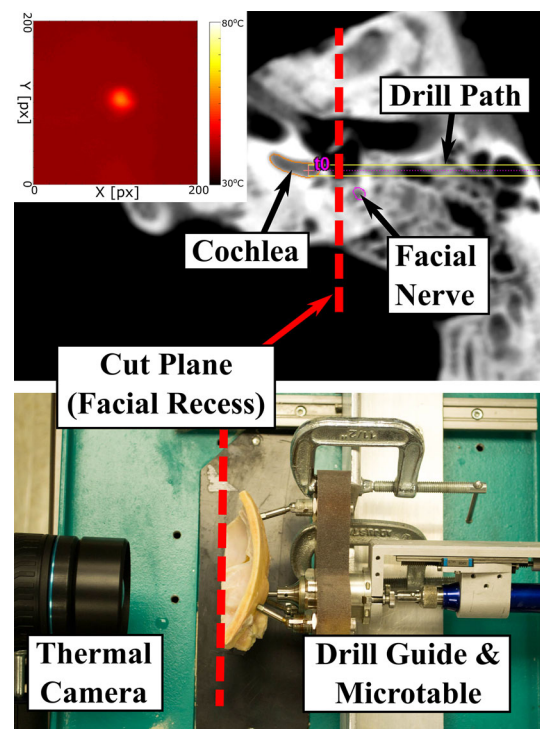

FIGURE 7. Experimental setup for evaluating temperature rise at the facial recess. (Top) CT scan of temporal bone specimen showing planned drill path (yellow), cochlea (orange), facial nerve (pink), and facial recess plane (red dashed line) where temperature recordings were made. (Bottom) Device hardware mounted to temporal bone and thermal camera positioned to record temperature during drilling at a plane located at the facial recess.

first trial was planned to follow the path that would be used for the surgery (from the skull surface to the cochlea). The subsequent trials were parallel to this first path and offset by several mm. All trials were performed at room temperature (~20 °C) so the temperature data was shifted upwards linearly to account for starting at approximately 37 °C in a clinical scenario. Custom drill bits made from hardened 440C stainless steel were used in these experiments (Orchid Orthopedic Solutions, Holt, MI, USA). Two drill bits are used in this procedure: a 3.8 mm, two-fluted twist drill bit for the wider, pilot hole and a 1.59 mm, three-fluted drill bit with CingleBit™ tip geometry for drilling through the facial recess. A new drill bit was used for each thermal monitoring experiment. Irrigation was performed per the protocol described in the previous section.

RESULTS

Four fresh temporal bones were used and three trials per bone were performed. The thermal camera malfunctioned for one of the trials so only 11 of the 12

trials provided usable data. Figure 8 shows the temperature data over time at the facial recess at distances of 0.5 and 1.0 mm from the edge of the drill for all trials. 0.5 mm represents a worst case scenario for the distance between the drill bit and the facial nerve. Paths are planned to be 0.6–0.7 mm from the nerve. Additional safety checks are employed throughout the surgery to determine if the drill is deviating from the path towards the facial nerve and the minimally invasive approach is aborted if necessary.

Of the 11 trials, 9 show temperature profiles that are below 50 °C for the entire drilling process at a distance of 0.5 mm from the drill path at the facial recess. Furthermore, the temperature is near 40 °C for the majority of the trial durations and the spikes above 45 °C are very brief. Two trials (Bone 1, Paths 1 and 2) had spikes in temperature that exceeded 60 °C. As will be explained in the discussion, the temperature profiles should be evaluated in terms of the total thermal dose, which accounts for the duration of time the bone spends at different temperatures.

The data was also analyzed according to the pre-operative protocol described in "Pre-operative Risk Assessment" section. The four temporal bone scans were analyzed and compared to each other and the prior clinical data set of nine patients[24] in terms of the two pre-operative risk metrics. The pre-operative scans indicate that Paths 1 and 2 of Bone 1 were at much higher risk than all other paths for excessive heat near the facial nerve, which is supported by the experimental results. In fact, when considering the CT images of the 13 specimens/patients in terms of the two patient-specific risk metrics described earlier, these paths stand out as being the riskiest according to bone intensity integral (7.5% for path 1 and 11.5% for path 2, where lower percentiles indicate higher risk). The thermal conductance metric can only be calculated for the first path for each bone since that is the only path that is planned in the standard location, approximately 0.6–0.7 mm from the facial nerve. Path 1 of Bone 1 ranked 11.5% for this metric. Table 2 provides the thermal metrics for all paths.

DISCUSSION

To evaluate the results from the various experimental trials and compare the data with estimates of temperature thresholds in the literature, the temperature response must be analyzed in terms of both temperature and exposure time. One common approach for quantifying tissue damage, which was originally used for measuring thermal doses for heat-based cancer therapies,[31] is to calculate the cumulative equivalent minutes at 43 °C (CEM43C):

$$\text{CEM43} = \int_0^{t_{\text{final}}} R(T(t))^{(43-T(t))} \mathrm{d}t$$

where $R(T(t)) = 0.5$ if $T(t) > 43\ °C$ and $R(T(t)) = 0.25$ otherwise. The equation is integrated over the time of tissue exposure and provides a metric that enables better comparison between various sets of transient temperature data and evaluation of likely tissue damage. According to this equation, as the temperature is increased by 1 °C, the exposure time must be decreased by a factor of two for the same thermal dose.

The temperature thresholds for different tissues vary considerably[34] and the threshold of the facial nerve is yet to be determined. There have been several prior studies evaluating the temperature tolerance of motor nerves, which can be used to estimate the tolerance of the facial nerve.[8,10,14,15,17,27] Table 3 provides a summary of these studies, along with the model used and their findings. The results vary substantially due to different animal models used (e.g. porcine laryngeal nerve, rat sciatic nerve) and heat application method (e.g. heated saline, high-intensity focused ultrasound).

Some studies suggest that nerves can be damaged at fairly low temperatures. For example, the work from De Vrind et al.[10] showed that rat sciatic nerve damage (decrease in function by at least 50%, as measured by electrophysiological examination) occurred in over 50% of the specimens when exposed to temperatures as low as 43 °C for 60–80 min. This temperature threshold is further supported by Haveman et al.[17] who concluded that peripheral nerve temperature should not exceed 44 °C for more than 30 min (CEM43C = 60 min).

Other studies present higher temperature thresholds for nerves. Lin et al. studied the electromyographic (EMG) response of porcine recurrent laryngeal nerves (RLN) after exposure to saline solutions at different temperatures/durations.[27] They concluded that 60 °C is a critical temperature for RLN thermal injury. In their experiments, no EMG change was measured at 55 °C after 60 s; however, damage occurred at 60 °C. At that temperature, nerve function was partially recoverable after 20 s (CEM43C = 4.37×10^4 min) and irrecoverable after 60 s (CEM43C = 1.31×10^5 min).

Perhaps the most relevant report related to estimating the threshold for facial nerve damage was completed by James et al.[17] While using their high-intensity focused ultrasound (HIFU) in the 1960s for destruction of vestibular organs in patients with Meniere's disease, they reported 2 out of 40 patients experienced facial nerve paralysis. They then measured
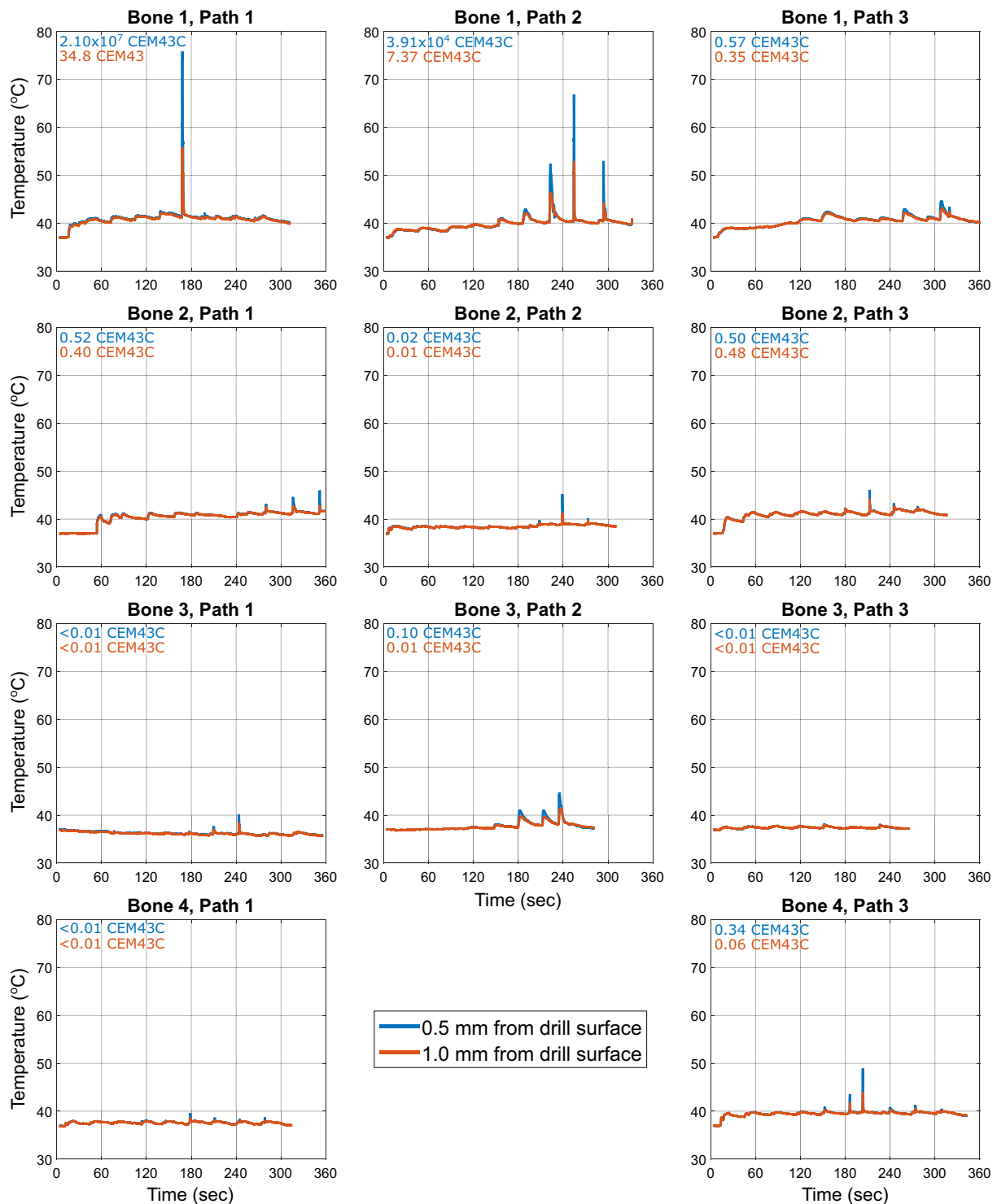
FIGURE 8. Temperature vs. time plots for 11 experimental trials using the revised drilling strategy described in "**Surgical Drilling Protocol for Reduced Heat Generation**" section. Temperature measurements are at the facial recess, where the drill passes closest to the facial nerve. The cumulative thermal dose in terms of equivalent minutes at 43 °C (CEM43) is also noted on the plots. Note that the thermal camera data acquisition malfunctioned for one trial so only two paths were analyzed for Bone 4.

the temperature at the facial nerve in cadaver temporal bones while using the HIFU at various power settings. At the power setting that was used in the previous 40

clinical cases (25 W/cm^2), the temperature was approximately 48 °C after a brief warm up period. They then lowered the power to 22 W/cm[22] for clinical

TABLE 2. Pre-operative risk metric values/ranks and thermal dose (CEM43C) for all trials.

| Bone | Path | Pre-operative risk metrics—risk percentile[a] | | CEM43C at dist. from drill[c] | | |
		Path intensity integral (%)	Thermal conductance[b] (%)	0.5 mm	0.75 mm	1.0 mm
1	1	7.70	11.5	2.10×10^7	1.12×10^4	34.8
	2	11.5		3.91×10^4	256.9	7.37
	3	26.9		0.57	0.44	0.35
2	1	46.2	73.1	0.52	0.43	0.40
	2	50.0		0.02	0.01	0.01
	3	50.0		0.50	0.49	0.48
3	1	53.8	96.2	<0.01	<0.01	<0.01
	2	50.0		0.10	0.03	0.01
	3	50.0		<0.01	<0.01	<0.01
4	1	38.5	84.6	<0.01	<0.01	<0.01
	2[d]	88.5		–	–	–
	3	65.4		0.34	0.10	0.06

[a]See "Pre-operative Risk Assessment" Section for description of each metric. Risk percentiles based on the scans of the four bones included in this study and the nine patients scans from Ref. 24 (lower percentile indicates greater risk).
[b]Only available for the Path 1 of each bone since this is the path planned through the facial recess, avoiding the nerves. Paths 2–3 were parallel to Path 1 at different distances to the nerve.
[c]Value calculated at various distances from the drill surface; mean temperature at each time step at a given distanced used in calculation.
[d]No thermal data for this trial due to a malfunction in the thermal camera recording software.

practice and no subsequent patients experienced facial paralysis (75 cases at the time of publication). This lower power corresponded to a temperature of 46 °C in the cadaver trials, which they concluded is the upper bound of facial nerve temperature tolerance. Of course, this conclusion does not incorporate the exposure duration. From their description of the ultrasound approach, it appears that the patients were exposed to the maximum power HIFU for approximately 10–20 min (CEM43C = 80–160 min).

Considering our experimental results in the context of the studies discussed above, all trials except for Paths 1 and 2 for Bone 1 have CEM43C values below 1 min and are considered to be safe according to even the most conservative criteria[15] when the nerve is 0.5 mm (and greater) from the drill surface. The two trials with higher peak temperatures are considered unsafe by all criteria discussed above if the nerve was 0.5 mm from the drill surface. Table 2 summarizes this data and the pre-operative risk metrics for each specimen.

It is important to note that the two cases in which temperature rose to potentially unsafe levels would have likely been excluded using the pre-operative screening protocol described in "Materials and Methods" section since this bone rated highest in both risk metrics out of the all bones in the data set (the four bones from this study and the nine prior patient scans[24]). An exact exclusion threshold is difficult to determine from this experimental data but given that these two paths were by far the highest risk of the data set, a reasonably conservative threshold (e.g. approximately 20–30%) would have excluded these paths. Using a conservative

threshold may result in excluding a patient/specimen unnecessarily (e.g. Bone 1, Path 3), but this is acceptable given the severity of potential complications. Thus, with a criteria of at least 20%, the thermal dose was at a safe level for the cases in which the minimally invasive approach would have been performed. This represents an important advancement over the prior clinical implementation, in which the pre-operative risk to thermal nerve injury did not appear to be related to the patient outcomes due to inconsistencies with the surgical approach. For example, the patient that experienced facial nerve palsy did not have extremely high risk metrics. Now, with a standardized drilling strategy, the higher risk patients per the pre-operative evaluation are associated with higher temperatures at the facial recess, enabling an effective criteria for exclusion.

Future work should focus on improving our surgical approach so the surgery can be safely performed on all patients. Potential areas of improvement include: optimized drill motor design to cut at a lower spindle speed and reduce heat generated by friction, optimized drill bit design (e.g. the single fluted drill bit design by Feldmann et al.[12]), and automated drill advancement with integrated force sensing. Additionally, more patient data should be acquired to determine the percentage of patients that would be excluded from the minimally invasive approach based on the criteria described in this paper as well as criteria described by Williamson et al.[33] that considers the facial recess dimensions and accuracy of the surgical system.

In conclusion, the revised surgical protocol for manual minimally invasive CI drilling, including the

Dillon *et al.*

TABLE 3. Prior research investigating temperature thresholds for neural injury.

Parameter	Control mode	Specification
Lin *et al.*[27]	Porcine recurrent laryngeal nerve; heated saline irrigation	EMG changes after 3 s exposure at 60°C, partially recoverable after 20 s, irrecoverable after 60 s (no EMG changes after 60 s at 55 °C)
Harnof *et al.*[14]	Porcine optic nerve; high-intensity focused ultrasound (HIFU)	Histologic evidence of thermal injury when exposed to 50–60°C for 6–10 s
Bunch *et al.*[8]	Canine phrenic nerve; radioablation catheter	Diaphragm motion impaired at 47 $\pm$ 3 °C with first onset at 20 s
De Vrind *et al.*[10]	Rat sciatic nerve; 5 mm segment of nerve heated with thermode	Temporary nerve damage at different exposure times at 43–45 °C; motor function recovered after 20 days
James *et al.*[17]	Temperature measured in at facial nerve in cadaver temporal bone with HIFU power levels that caused facial paralysis	46 °C determined to be temperature associated with ultrasound intensity of 22 W/cm^2, which did not cause facial paralysis when used clinically (no surgical exposure time given)

pre-operative scanning step and the improved drilling strategy enables safer implementation of this surgery in cases in which the patient is not pre-disposed to high risk of thermal injury. The exclusion criterion appears to be effective, especially if used conservatively; however, more patient data needs to be considered to provide better estimates of patient risk and determine a more precise cut-off point.

ACKNOWLEDGMENTS

REFERENCES

[1]Ansó, J., C. Dür, K. Gavaghan, H. Rohrbach, N. Gerber, T. Williamson, E. M. Calvo, T. W. Balmer, C. Precht, D. Ferrario, and M. S. Dettmer. A neuromonitoring approach to facial nerve preservation during image-guided robotic cochlear implantation. *Otol. Neurotol.* 37(1):89–98, 2016.

[2]Bağci, E., and B. Ozcelik. Investigation of the effect of drilling conditions on the twist drill temperature during step-by-step and continuous dry drilling. *Mater. Des.* 27(6):446–454, 2006.

[3]Balachandran, R., J. E. Mitchell, G. Blachon, J. H. Noble, B. M. Dawant, J. M. Fitzpatrick, and R. F. Labadie. Percutaneous cochlear implant drilling *via* customized frames: an in vitro study. *Otolaryngol. Head Neck Surg.* 142(3):421–426, 2010.

[4]Baron, S., H. Eilers, B. Munske, J. L. Toennies, R. Balachandran, R. F. Labadie, T. Ortmaier, and R. J. Webster, III. Percutaneous inner-ear access *via* an image-guided industrial robot system. *Proc. Inst. Mech. Eng. H* 224(5):633–649, 2010.

[5]Bell, B., N. Gerber, T. Williamson, K. Gavaghan, W. Wimmer, M. Caversaccio, and S. Weber. In vitro accuracy evaluation of image-guided robot system for direct cochlear access. *Otol. Neurotol.* 34(7):1284–1290, 2013.

[6]Bell, B., C. Stieger, N. Gerber, A. Arnold, C. Nauer, V. Hamacher, M. Kompis, L. Nolte, M. Caversaccio, and S. Weber. A self-developed and constructed robot for minimally invasive cochlear implantation. *Acta Otolaryngol.* 132(4):355–360, 2012.

[7]Bertollo N, WR Walsh (2011) Drilling of bone: practicality, limitations and complications associated with surgical drill-bits. In: Biomechanics in Applications, edited by V Klika. InTech. doi: 10.5772/20931.

[8]Bunch, T. J., G. K. Bruce, S. Mahapatra, S. B. Johnson, D. V. Miller, A. V. Sarabanda, M. A. Milton, and D. L. Packer. Mechanisms of phrenic nerve injury during radiofrequency ablation at the pulmonary vein orifice. *J. Cardiovasc. Electrophysiol.* 16(12):1318–1325, 2005.

[9]Davidson, S. R., and D. F. James. Measurement of thermal conductivity of bovine cortical bone. *Med. Eng. Phys.* 22(10):741–747, 2000.

[10]De Vrind, H. H., J. Wondergem, and J. Haveman. Hyperthermia-induced damage to rat sciatic nerve assessed in vivo with functional methods and with electrophysiology. *J. Neurosci. Methods* 45(3):165–174, 1992.

[11]Feldmann, A., J. Anso, B. Bell, T. Williamson, K. Gavaghan, N. Gerber, H. Rohrbach, S. Weber, and P. Zysset. Temperature prediction model for bone drilling based on density distribution and in vivo experiments for minimally invasive robotic cochlear implantation. *Ann. Biomed. Eng.* 44(5):1576–1586, 2016.

[12]Feldmann, A., J. Wandal, and P. Zysset. Reducing temperature elevation of robotic bone drilling. *Med. Eng. Phys.* 38(12):1495–1504, 2016.

[13]Feldmann, A., and P. Zysset. Experimental determination of the emissivity of bone. *Med. Eng. Phys.* 38(10):1136–1138, 2016.

[14]Harnof, S., Z. Zibly, Z. Cohen, A. Shaw, C. Schlaff, and N. F. Kassel. Cranial nerve threshold for thermal injury induced by MRI-guided high-intensity focused ultrasound (MRgHIFU): preliminary results on an optic nerve model. *IEEE Trans. Ultrason. Ferroelectr Freq Control* 60(4):702–705, 2013.

[15]Haveman, J., J. Van Der Zee, J. Wondergem, J. F. Hoogeveen, and M. C. Hulshof. Effects of hyperthermia on the peripheral nervous system: a review. *Int. J. Hyperth.* 20(4):371–391, 2004.

[16]House, J. W., and D. E. Brackmann. Facial nerve grading system. *Otolaryngol. Head Neck Surg.* 93(2):146–147, 1985.

[17]James, J. A., G. A. Dalton, H. F. Freundlich, M. A. Bullen, P. N. Wells, D. A. Hughes, and J. Chow. Histological, thermal and biochemical effects of ultrasound on the labyrinth and temporal bone. *Acta Otolaryngol.* 57(3–6):306–312, 1964.

[18]Kim, D. W., Y. S. Lee, M. S. Park, and C. N. Chu. Tool life improvement by peck drilling and thrust force monitoring during deep-micro-hole drilling of steel. *Int. J. Mach. Tools Manuf.* 49(3):246–255, 2009.

[19]Kobler, J. P., J. Kotlarski, J. Öltjen, S. Baron, and T. Ortmaier. Design and analysis of a head-mounted parallel kinematic device for skull surgery. *Int. J. Comput. Assist. Radiol. Surg.* 7(1):137–149, 2012.

[20]Kobler, J. P., K. Nuelle, G. J. Lexow, T. S. Rau, O. Majdani, L. A. Kahrs, J. Kotlarski, and T. Ortmaier. Configuration optimization and experimental accuracy evaluation of a bone-attached, parallel robot for skull surgery. *Int. J. Comput. Assist. Radiol. Surg.* 11(3):421–436, 2016.

[21]Kratchman, L. B., G. S. Blachon, T. J. Withrow, R. Balachandran, R. F. Labadie, and R. J. Webster. Design of a bone-attached parallel robot for percutaneous cochlear implantation. *IEEE Trans. Biomed. Eng.* 58(10):2904–2910, 2011.

[22]Kronenberg, J., W. Baumgartner, L. Migirov, T. Dagan, and M. Hildesheimer. The suprameatal approach: an alternative surgical approach to cochlear implantation. *Otol. Neurotol.* 25(1):41–45, 2004.

[23]Kronenberg, J., L. Migirov, and T. Dagan. Suprameatal approach: new surgical approach for cochlear implantation. *J. Laryngol. Otol.* 115(04):283–285, 2001.

[24]Labadie, R. F., R. Balachandran, J. H. Noble, G. S. Blachon, J. E. Mitchell, F. A. Reda, B. M. Dawant, and J. M. Fitzpatrick. Minimally invasive image-guided cochlear implantation surgery: first report of clinical implementation. *Laryngoscope* 124(8):1915–1922, 2014.

[25]Labadie, R. F., J. Mitchell, R. Balachandran, and J. M. Fitzpatrick. Customized, rapid-production microstereotactic table for surgical targeting: description of concept and in vitro validation. *Int. J. Comput. Assist. Radiol. Surg.* 4(3):273–280, 2009.

[26]Lee, J., O. B. Ozdoganlar, and T. Rabin. An experimental investigation on thermal exposure during bone drilling. *Med. Eng. Phys.* 34:1510–1520, 2012.

[27]Lin, Y. C., G. Dionigi, G. W. Randolph, I. Lu, P. Y. Chang, S. Y. Tsai, H. Y. Kim, H. Y. Lee, R. P. Tufano, H. Sun, and X. Liu. Electrophysiologic monitoring correlates of recurrent laryngeal nerve heat thermal injury in a porcine model. *Laryngoscope* 125(8):E283–E290, 2015.

[28]Majdani, O., T. S. Rau, S. Baron, H. Eilers, C. Baier, B. Heimann, T. Ortmaier, S. Bartling, T. Lenarz, and M. Leinung. A robot-guided minimally invasive approach for cochlear implant surgery: preliminary results of a temporal bone study. *Int. J. Comput. Assist. Radiol. Surg.* 4(5):475–486, 2009.

[29]Noble, J. H., O. Majdani, R. F. Labadie, B. Dawant, and J. M. Fitzpatrick. Automatic determination of optimal linear drilling trajectories for cochlear access accounting for drill-positioning error. *Int. J. Med. Robot.* 6(3):281–290, 2010.

[30]Noble, J. H., F. M. Warren, R. F. Labadie, and B. M. Dawant. Automatic segmentation of the facial nerve and chorda tympani in CT images using spatially dependent feature values. *Med. Phys.* 35(12):5375–5384, 2008.

[31]Sapareto, S. A., and W. C. Dewey. Thermal dose determination in cancer therapy. *Int. J. Radiat. Oncol. Biol. Phys.* 10(6):787–800, 1984.

[32]Williamson, T. M., B. J. Bell, N. Gerber, L. Salas, P. Zysset, M. Caversaccio, and S. Weber. Estimation of tool pose based on force–density correlation during robotic drilling. *IEEE Trans. Biomed. Eng.* 60(4):969–976, 2013.

[33]Williamson, T., K. Gavaghan, N. Gerber, S. Weder, L. Anschuetz, F. Wagner, C. Weisstanner, G. Mantokoudis, M. Caversaccio, and S. Weber. A population statistics approach for safety assessment in robotic cochlear implantation. *Otol. Neurotol.* 38(5):759–764, 2016.

[34]Yarmolenko, P. S., E. J. Moon, C. Landon, A. Manzoo, D. W. Hochman, B. L. Viglianti, and M. W. Dewhirst. Thresholds for thermal damage to normal tissues: an update. *Int. J. Hyperth.* 27(4):320–343, 2011.